CLAS-NOTE 2004-039
CVS: docs/clas_notes/0knurep090604
Original: September 24, 2004

Studies of time resolution of the Burle 85001 micro-channel plate photo-multipliers in comparison with standard PMTs

Status Report of TOF Studies
at Kyungpook National University
in 2004

V.N. Batourine, W. Kim,
S. Majewsky, V. Popov,
E.S. Smith, D. Son, and C. Zorn

Abstract

In continuation of CLAS note 2004-16 we present updated results on the measurements of the PMT timing resolution. The cosmic ray method utilizing six identical PMTs $R2083$ from Hamamtsu and three scintillating counters $(2 \times 3.3 \times 50)\ cm^3$ from Bicron was used to determine $\sigma_{R2083} = 56.6 \pm 0.7\ ps$. The measurement method of coordinates of β-particles emitted by the radiative source at known locations has been used for comparison of $R2083$ and micro-channel plate PMs $Burle - 85001$. This method requires only one counter with two PMs at both ends. This method yields $\sigma_{R2083} = 59.5 \pm 0.7\ ps$ in agreement with the cosmic ray method. For the micro-channel plate PMs with the external amplification of 10 to the signals this method yields $\sigma_{85001} = 130 \pm 4\ ps$.

Introduction

The timing information in CLAS experiments[1] has been taken from both ends of extended scintillators. In such a case the standard deviation of TOF between two identical counters is equal to σ_{PMT}(assuming equal resolutions for all PMTs). Hence, the main goal of our studies at KNU is to develop a prototype for the time-zero counter providing the effective resolution $\sigma_{PMT} \leq 50\ ps$ for minimum ionizing particles. We refer to σ_{PMT} as an "effective resolution" in order to emphasize that this value is defined not only by the characteristics of PMTs, but by the experimental environments, as well. In particular, the barrel structure of 56 time-zero scintillators is expected to be placed in the area of a high magnetic field $B \geq 2T$. It is well known that magnetic fields significantly reduce amplitudes of signals and deteriorate the timing resolution, as well.

If ordinary dynode PMTs are in use then the only way to exclude the influence of the magnetic field is to move PMs out of the region of high magnetic field. Therefore, $\approx 1m$ long light guides are required to deliver the light to photo-cathodes.

In our previous note[2] we have shown that σ_{R2083} may be as good as $\approx 60\ ps$, conditioned by that two PMTs are attached directly to the ends of "Bicron-408" scintillator($2 \times 3.3 \times 50\ cm^3$). These measurements were done with two different methods[2]. In the first method reconstructed tracks of cosmic particles has been used to deduce σ_{PMT}. This method requires 3 identical counters instrumented with 6 identical PMTs. The second method is the coordinate method in which the resolution of PMT has been determined from coordinate distribution of light flashes around the known location of the lionization source. The longitudinal coordinates were measured with only 2 identical PMTs, attached to the ends of scintillator. We present the updated values of σ_{PMT} obtained with 3 kinds of photo-multipliers in Section-2.

The next logical step in the prototype development and studies is to measure the effective resolution via $1m$ long light guides. Our first tests with *air light guides* have shown that the amount of light on photo-cathodes is not enough for precise timing, even when the signals are amplified for further discriminating and processing. Therefore, we immediately began to design and produce two acrylic light guides with length $1m$. These tests will be of crucial importance for such approach.

We consider possible alternatives to the design with long light guides. One of them could be the implementation of micro-channel plate PMs the performance of which were tested[3] in magnetic fields up to $2T$. Due to the immunity of MCPs to magnetic fields[3] MCP PMs could be attached directly to scintillators. Since the MCP transition time is short, the single electron resolution of MCP may be as good as $\approx 30\ ps$[3]. However, at such level of accuracy, the resolution of scintillation counters is mostly dictated by statistical fluctuations of photon's timing. In order to estimate how well MCP PMs match to the requirements of the CLAS experiment we have performed several tests with the setup of the same scintillator and *two* MCP PMs "Burle-85001". Only the coordinate method is available for such tests. Other methods require more than two identical PMs. Therefore, we describe the coordinate method in detail below.

1 Coordinate method for the measurements of PMT resolution.

We have developed the so-called "coordinate method" for measuring the effective PMT resolution. This method requires only one scintillating counter with two identical PMTs attached to its ends. The resolution of PMT has been determined from the residuals of measured coordinates of ionizing particles from the radiative source at known location. The source size ($\sigma \approx 3mm$) may be neglected[2].

X-coordinate method. The method is based on the simple relation between the light flash coordinate x and arrival times, t_l and t_r, of signals from two PMTs, located at the ends of an extended scintillator:

$$t_x = t_l - t_r = \frac{2x}{c_s} + const, \tag{1}$$

where x is the coordinate of the light flash, t_x is the value digitized by TDC, c_s is the effective speed of light in scintillating media, l is the length of scintillator; *const* accounts for all kinds of propagation delays.

The standard deviation of t_x relates to the individual left and right PMT resolutions as

$$\langle(\delta t_x)^2\rangle = \langle(\delta t_l)^2\rangle + \langle(\delta t_r)^2\rangle + \langle(\delta t_{TDC})^2\rangle + \left(\frac{2}{c_s}\right)^2 \langle(\delta x)^2\rangle \tag{2}$$

where $\langle(\delta t_{l,r})^2\rangle$ are the timing standard deviations for left or right PMTs; we assume that $\langle(\delta t_l)^2\rangle = \langle(\delta t_l)^2\rangle = \sigma^2_{PMT}$, $\langle(\delta t_{TDC})^2\rangle$ is the intrinsic resolution of the TDC, $\langle(\delta x)^2\rangle$ represents the size of the radiation source.

The ionization with known coordinate may be provided with a narrow beam of β-particles from the ionization source. Thus, from this formula one can determine the single PMT resolution as

$$\sigma_{PMT} = \frac{1}{\sqrt{2}}\sqrt{\langle(\delta t_x)^2\rangle - \langle(\delta t_{TDC})^2\rangle - \left(\frac{2}{c_s}\right)^2\langle(\delta x)^2\rangle} \tag{3}$$

We illustrate the coordinate method in Fig. 1, in which we show two images of the radiative source in the X-coordinate scale. These images were accumulated with two R2083 PMs from Hamamatsu at two “off-line” energy thresholds for β-particles. The longitudinal coordinates of β-particles has been determined by Eq. (1). The peaks at about zero indicate the ionization source placed in the middle of the counter. The 50 *cm* wide plateau is the manifestation of cosmic particles spanned by the counter.

$X+$ method: extrapolation of energy dependent σ to M.I.P.'s ionization. From the off-line analysis of the data files accumulated with the radiation source we have determined the dependence of the PMT resolution upon the energy of β-particles. Typical outcomes of such studies are shown in Fig. 2 and Fig. 3. Each of these two figures contains plots for one of two source locations: $+15$ *cm* and -15 *cm*, respectively. Below we explain the contents of each panel referred to as “(raw-column)”.

- (1-1).Energy(E) spectra of β-particles. The energy of β-particles has been determined as

  $$E = k\sqrt{(a_l - p_l)(a_r - p_r)} \tag{4}$$

  where $a_{l,r}$ and $p_{l,r}$ are the amplitudes and pedestals from ADCs corresponding to left or right sides of the counter; k is the calibrating factor. The last has been determined from the fit of the β-spectrum by the formula

  $$n(\varepsilon) = G(\sigma,\mu)(\varepsilon)\sqrt{(\varepsilon^2 - 1)}(\varepsilon_0 - \varepsilon)^2 \tag{5}$$

  where $\varepsilon = E/m_ec^2$, $n(\varepsilon)$ is the number of events with specified ε, ε_0=2.28 MeV/m_ec^2 specifies the upper limit of the β-spectrum, G stands for a Gaussian.

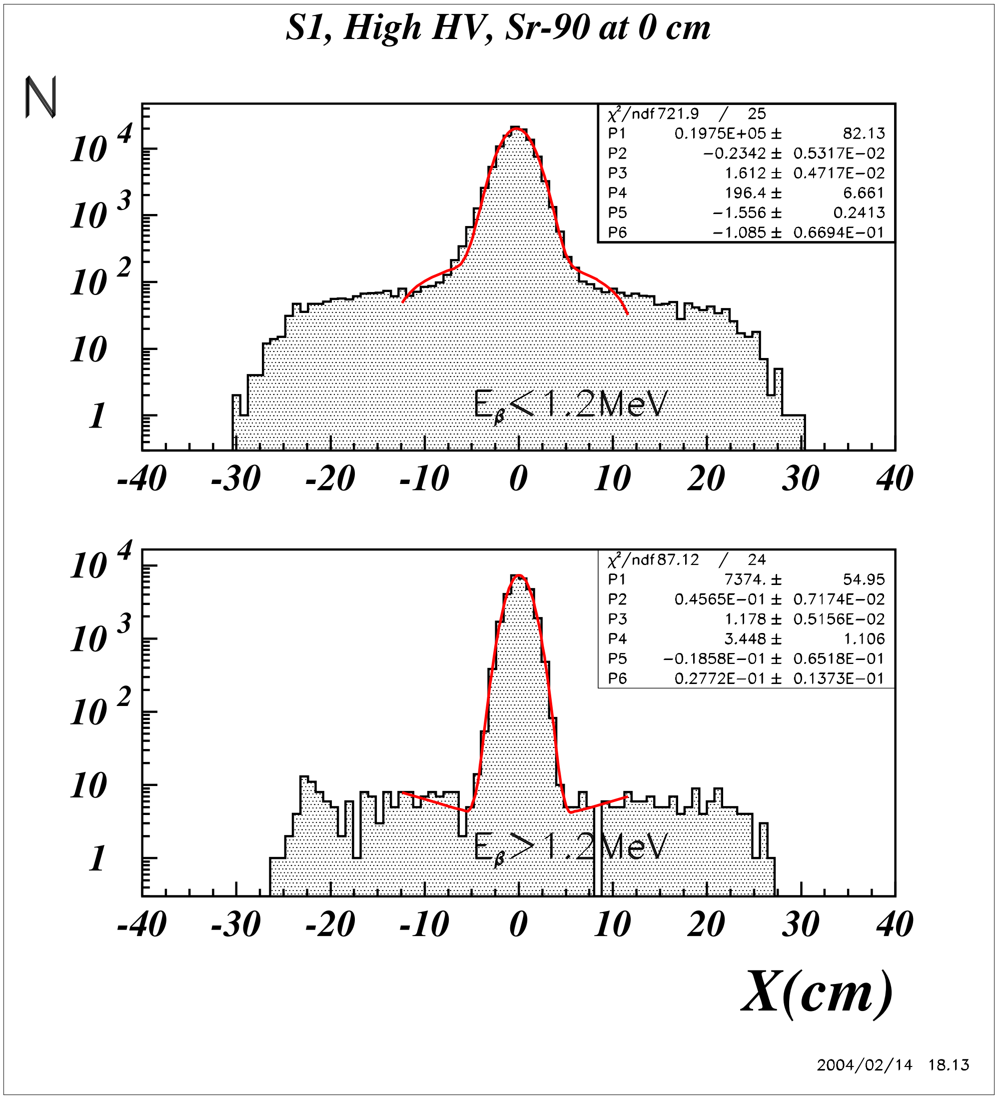

Figure 1: The "β-ray" images of ^{90}Sr source in two energy intervals of β-particles. Top panel - $E_\beta < 1.2\ MeV$. Bottom panel- $E_\beta > 1.2\ MeV$.

- (2-1).The distribution of events over the longitudinal coordinate X defined by Eq. 1 in ns. The peak at zero is the image of the source.

  Scatter plots X vs E has been also created for both locations. The energy slices 100 KeV wide has been fitted then by a Gaussian. Thus, the dependence $\sigma_X(E)$ has been measured. It is shown in the next panel.

- (1-2).Energy dependences $\sigma_X(E)$. As one can see from these plots σ_X varies as $1/\sqrt{E}$. Obviously this behavior is due to the increase of the signal-to-noise ratio. Extrapolating $\sigma_X(E)$ to the energy deposit of minimum ionizing particles $E_{MIP} = 4.4\ MeV$ one can estimate the effective value of a PMT resolution for M.I.P.s(σ_{MIP}).

- (2-2).The energy dependence of the center of the ^{90}Sr image $\langle X\rangle(E)$. The attention should be paid to the fact that there are obviously opposite displacements of both source images with decreasing energy.

Method for measurements of the number of primary photo-electrons. The following method has been used for estimating the number of primary photoelectrons. We define two energies *measured* from two sides of the counter: $e_{1,2}(E) = k_{1,2} \times (a_{1,2} - p_{1,2})$, where $k_{1,2}, a_{1,2}, p_{1,2}$ are the corresponding calibrating factors, ADC values and pedestals, respectively. Both values are functions of the original energy deposit in the scintillator E. We determine the total *measured* energy deposit e and the difference of two energies Δe as

$$e(E) = e_1(E) + e_2(E) \quad and \quad \Delta e(E) = e_1(E) - e_2(E) \tag{6}$$

For the standard deviations of both values, defined above, we find

$$\sigma^2_{\Delta e} = \sigma^2_e = \langle(\delta e_1(E))^2\rangle + \langle(\delta e_2(E))^2\rangle \tag{7}$$

where σ_e is the standard deviation of the energy deposit measured from both sides of the counter. It is obvious that

$$\frac{\sigma_e}{e} = \frac{\sqrt{N(E)}}{N(E)}, \tag{8}$$

where $N(E)$ is the number of primary photoelectrons produced by a particle depositing energy E in *both* PMTs. Therefore, the energy dependent number

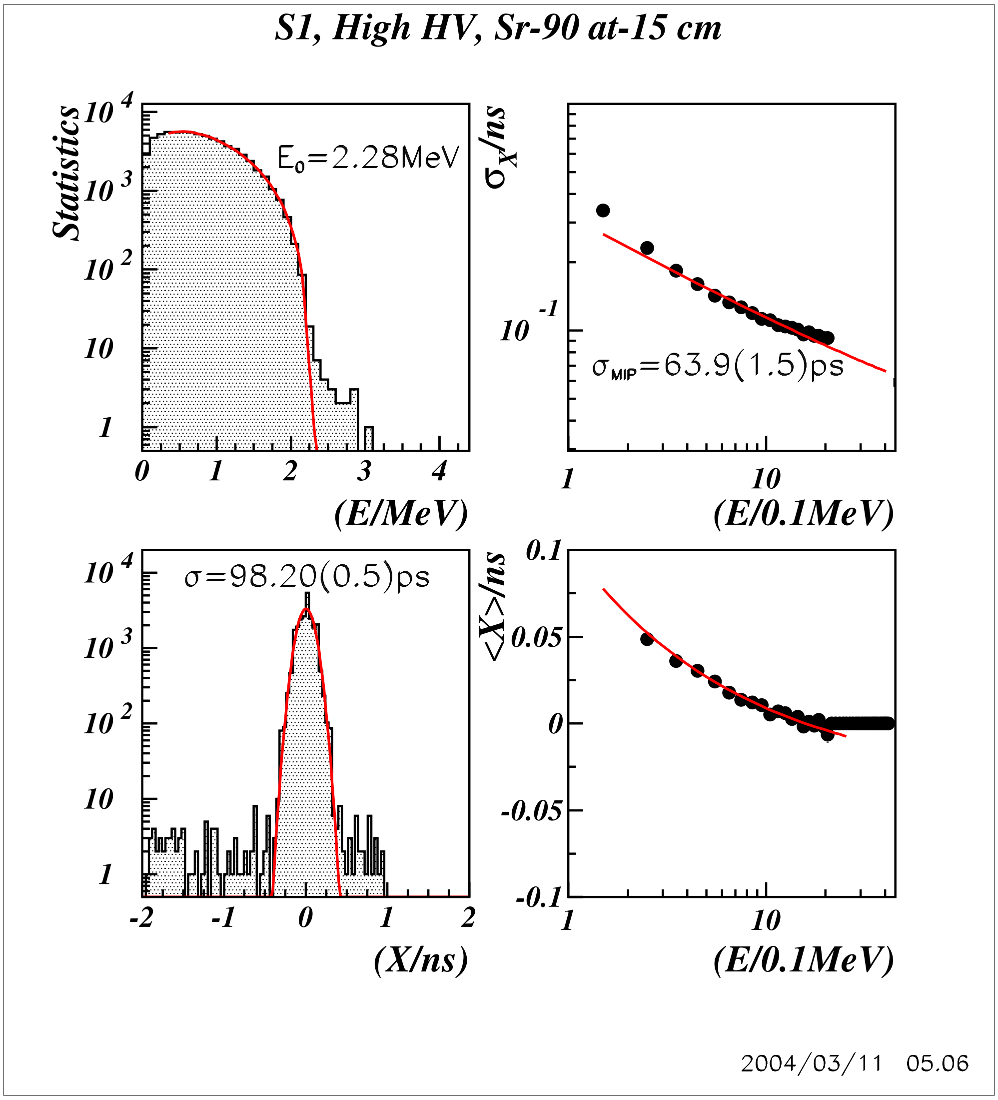

Figure 2: $X+$ method for $R2083$ from Hamamatsu at ^{90}Sr location -15 cm. Panel: (1-1) - energy (E) spectrum of β-particles ; (2-1) - coordinate(X) spectrum of β-particles; (1-2) - σ_X of the peak vs β-particle energy(E); (2-2) - $\langle X\rangle$ of the peak vs β-particle energy(E). The position of peak on the X-scale was adjusted to zero for convenience.

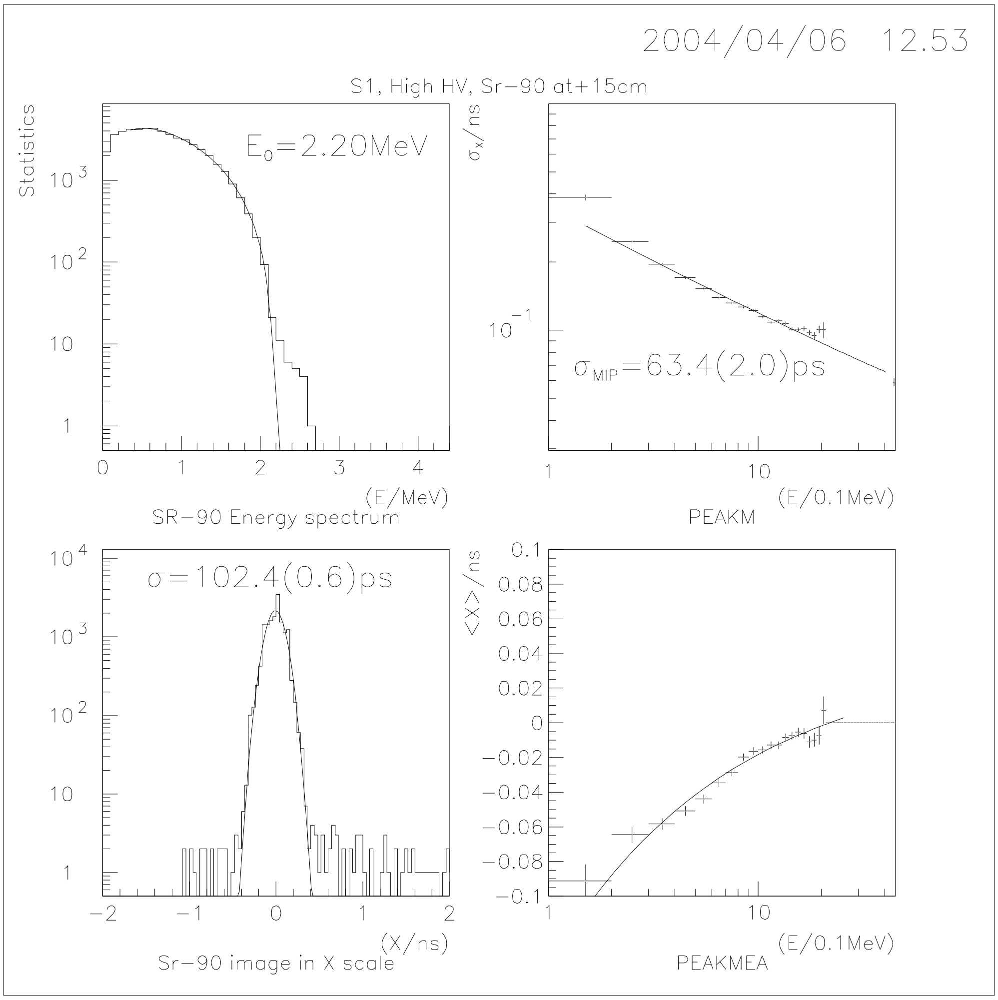

Figure 3: $X+$ method for $R2083$ from Hamamatsu at ^{90}Sr locations $+15\ cm$. Panel: (1-1) - energy (E) spectrum of β-particles ; (2-1) - coordinate(X) spectrum of β-particles; (1-2) - σ_X of the peak vs β-particle energy(E); (2-2) - $\langle X\rangle$ of the peak vs β-particle energy(E). The position of peak on the X-scale was adjusted to zero for convenience.

of primary photoelectrons may be determined as

$$N(E) = \left(\frac{e(E)}{\sigma_e(E)}\right)^2 = \left(\frac{e(E)}{\sigma_{\Delta e}(E)}\right)^2 \tag{9}$$

It is not possible to measure σ_e with the continuous energy spectrum. However, by measuring Δe distribution and using the fact that $\sigma_{\Delta e}$=σ_e (see Eq. 7) one can determine σ_e in Eq. 9. Hence, $N(E)$ may be determined with *measured* $\sigma_{\Delta e}$ and $e(E)$. The function $\sigma_{\Delta e}(E)$ has been determined via the scatter plot of E.vs.$\Delta e(E)$.

The resulting function $N(E)$, determined via Eq. 9, is shown in Fig. 4. We consider that the predicted for M.I.Ps number $N_{ppe} = 686 \pm 10$ for our $2 \times 3.3 \times 50\ cm^3$ scintillator is in agreement with the $N_{ppe} = 1000 \pm 100$ determined for TOF counters[1] of CLAS experiments sized as $5.1 \times 15 \times 32.3\ cm^3$. The first N_{ppe}-value is supposed to be emitted from *two* photo-cathodes of R2083, the sensitivity of which is of 80 μA/lm. The second value corresponds to *one* photo-cathode of $EMI - 9954B05$ photo-multiplier with the sensitivity of 110 μA/lm. If scaled to the thickness of our scintillator ($\times 0.4$) and cathode sensitivity ($\times 0.727$) ,the second number turns to 582 ± 58 for *two* photo-cathodes of $EMI - 9954B05$, which matches quite well to the first value.

Advantages of the coordinate method. The coordinate method has several important advantages. Firstly, it requires only one counter instrumented with two identical PMTs. Secondly, the data taking and data analysis up to the final value takes only several minutes. Finally, this method is free from the systematics related to the coordinate dependence of signal's timing, since the ionization is localized in known narrow area of $\pm 0.3\ cm$. Moreover, the coordinate method may be used for studies of the coordinate dependent systematics. The last may be measuring directly at different locations of the ionizing source. This method may be also used as an express "on-line" method for studies of the PMT resolution in different environments.

Since the yielding value of σ_{PMT} is inversely proportional to $\sqrt{E_\beta}$ the "on-line" result of this method will be noticeably better if the ionization source $^{106}Ru(E_\beta^{max} = 3.541\ MeV)$ is implemented.

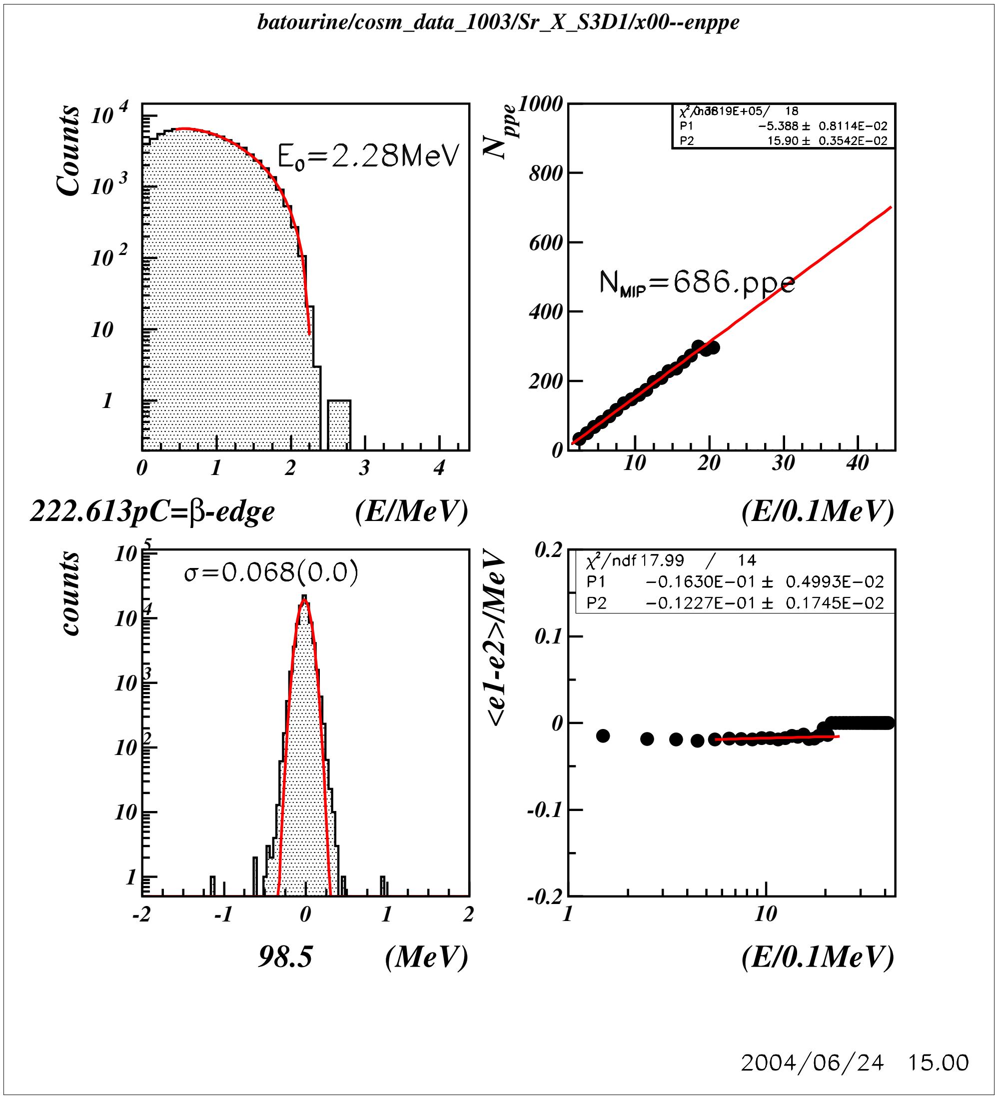

Figure 4: (1-1):energy (E) spectrum of β-particles.
(1-2):energy dependence of the number of primary photoelectrons $N_{ppe}(E)$. It is s expected to be 686 ± 10 at MIP energy of $\approx 4.4\ MeV$.
(2-1):spectrum of $(e_1 - e_2)$, where $e_{1,2}$ are the energies measured from two sides of the counter.
(2-2):mean value of $(e_1 - e_2)$ vs energy (E) of β-particles.

2 Current status of the resolution measurements.

In our notes[2] we discussed several approaches for measuring σ_{PMT}. The updated values of σ_{PMT} resulting from different methods are shown in the Table 1.

Method	Acceptance	Particles	ΔE	σ_{PMT}
$X+$ R2083	$< local >$	$\beta from ^{90}Sr$ $E_\beta < 2.28\ MeV$	$extrapolated$ $\approx 4.4\ MeV$	59.5±0.7 ps
$X+$ MCP 85001	$< local >$	$\beta from ^{90}Sr$ $E_\beta < 2.28\ MeV$	$extrapolated$ $\approx 4.4\ MeV$	130.±4. ps
6 PMTs R2083 tracking	$0 \pm 25\ cm$	cosmic	4.4 MeV	61.1±0.6 ps
6 PMTs R2083 tracking	$< local >$	cosmic	4.4 MeV	56.6±0.7 ps

Table 1: PMT resolution(standard deviation) from different methods. The errors shown in this table are yielded by fitting procedures. We estimate a possible systematic error to be of about +4.4% to the shown values.

The local σ_{PMT} from the tracking method with 3 counters (6 PMTs) is now in good agreement to the local X-coordinate method. The middle counter is now instrumented with the CFDs, which was leased by JLAB. We also observe now a quite stable behavior of the resolution upon the time.

We emphasize that the results shown in Table 1 were obtained with the prototype, which has no light guides. The actual conditions for the light collection will be significantly worse. Therefore, we consider these values as the most optimistic limit of σ_{PMT}.

A good agreement between σ_{PMT}'s from the cosmic ray method (6 PMT tracking method) and coordinate method with extrapolation to higher energies ($X+$ method) ensures that $X+$ method is an adequate tool for measuring of σ_{PMT} at M.I.P. energy.

Study of σ_{PMT} vs HV via the $X+$ method. We have measured the dependence of σ_{PMT} upon the HV. We adjusted the amplitudes of signals from both sides to be equal to the given value. The dependence of the resolution upon the amplitudes of signals is shown in Fig. 5. One can see that the resolution gradually improves up to the HV corresponding to the averaged signal amplitude of 900 mV. Above this value almost no change in the resolution can be seen. It is quite surprising that the resolution does not improve with the increasing signal/noise ratio. Perhaps, such behavior indicates some noise related to the HV circuit.

Study of σ_{PMT} vs X-coordinate. In order to study the systematics of PMT timing we have measured the dependence of both σ_{PMT} and peak location upon X-coordinate. We adjusted the amplitudes of signals from both sides to be equal to the given value at the center of the counter. The dependence of the resolution upon X-coordinate of the lionization source is shown in Fig. 6. These data were obtained with *high* HVs=(2350V,2500V). One can see from this figure that the resolution oscillates near the mean value of 59.5 ± 0.7 ps with the period of about 25 cm.

Comparison with EMI9813B PMTs. We have measured the timing resolution for EMI-9813B PMT. The results are shown in Fig. 8 at *high* voltages (1770V,1710V) and Fig. 9 at *low* voltages (1700V,1650V). Such kind of PMTs has been used in the time-of-flight system for CLAS[**?**]. The resolution measured with X+ method agrees with the previously measured values[1]. Compared to the resolution of R2083 PMT of Hamamatsu, the standard deviation of EMI-9813B timing is ≈ 10 ps wider. This could be due to the transit time spread of these PMTs.

σ_{PMT} from cosmic ray measurements with 6 PMTs. In our previous measurements we found the long term instability in one of our counters, which was instrumented with the CAEN leading edge discriminators. We replaced this discriminators by the constant fraction discriminators Philips-715. Both the stability and resolution, yielded from the 6 PMT method, are significantly better now. The result from the 6PMT method is shown in Fig. 10. The local resolution(within the bin of about 2.5 cm wide) has been determined to be of 56.3 ± 0.7 ps. The overall resolution yielded by this method is of 61.5 ± 0.6 ps. The overall resolution is worse of the local value

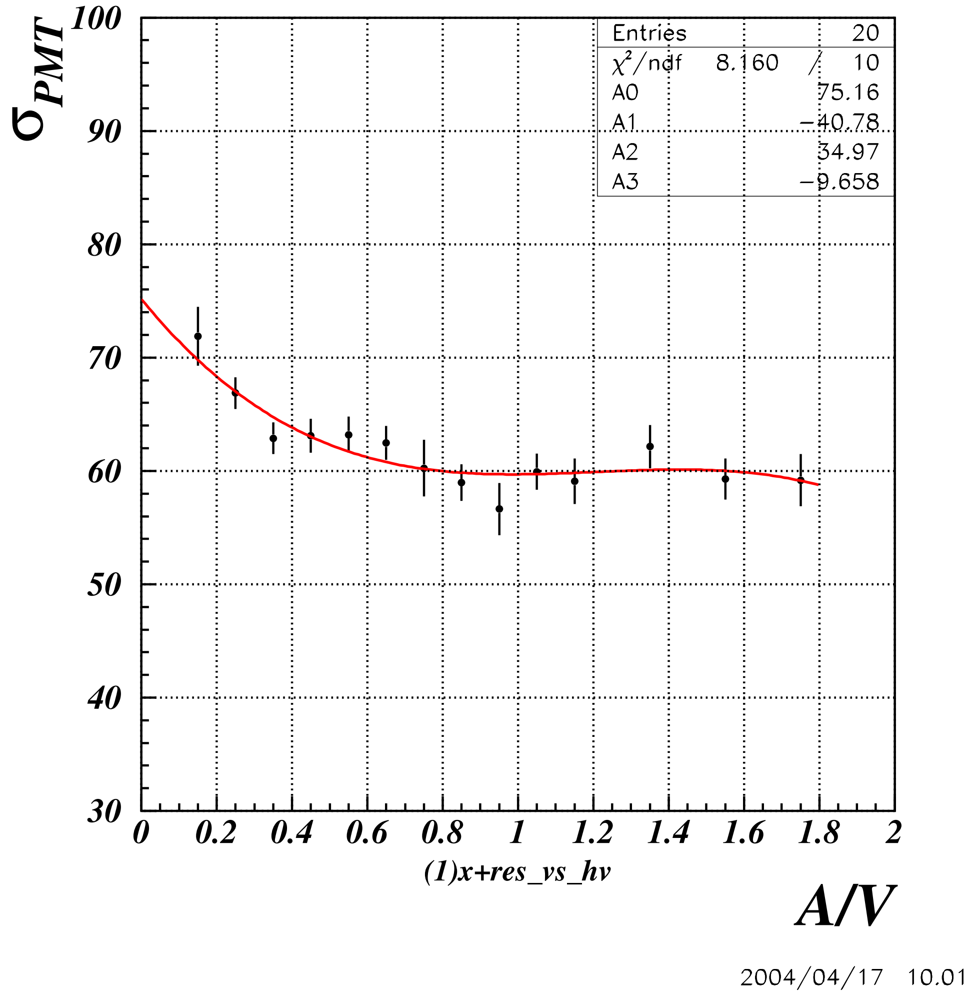

Figure 5: The dependence of σ_{PMT} yielded by the $X+$ method upon the signal amplitude A. Amplitude A has been measured via the scope. The mean value of σ_{PMT} in the plateau region $(0.9, 1.8V)$ is of 59.5 ± 0.7 ps.

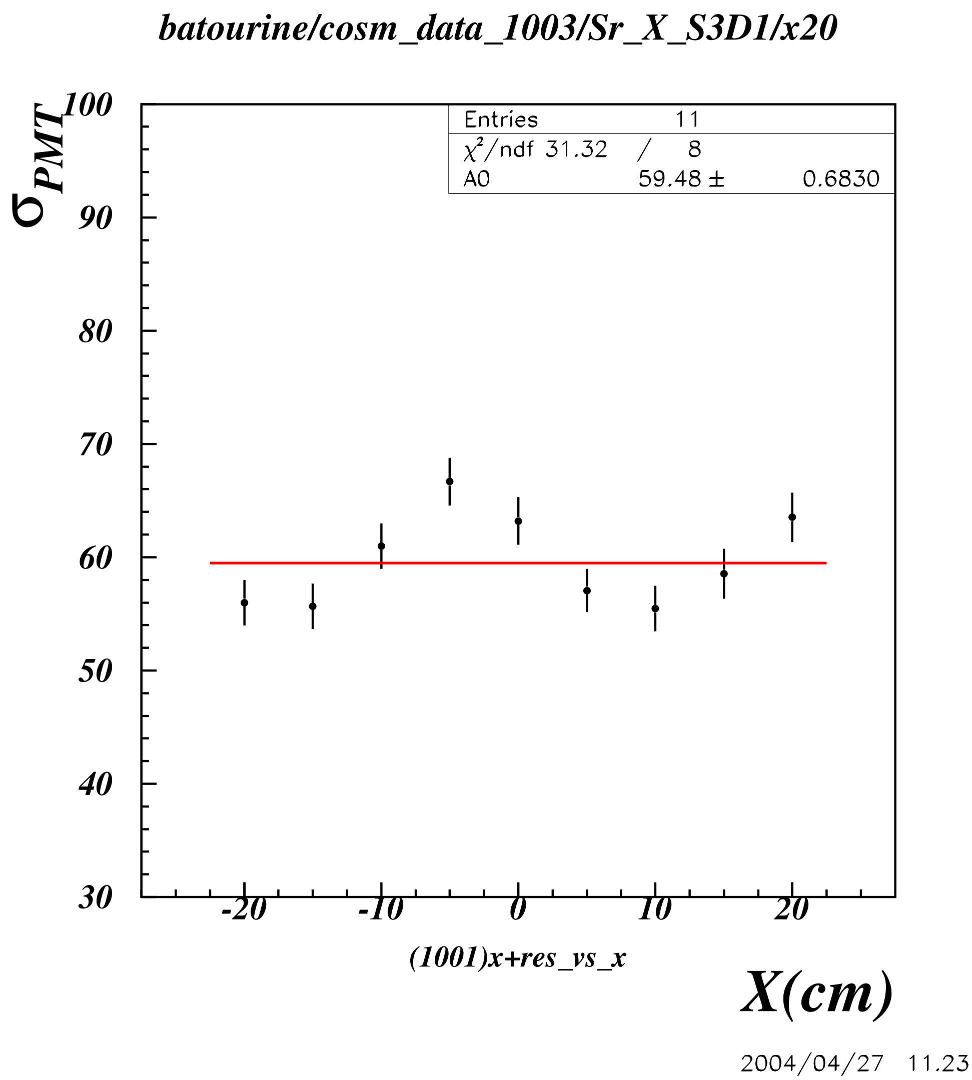

Figure 6: The dependence of σ_{PMT} yielded by the $X+$ method upon X-coordinate at *high* $HV(2370V, 2500V)$. The averaged value is 59.5 ± 0.7 ps.

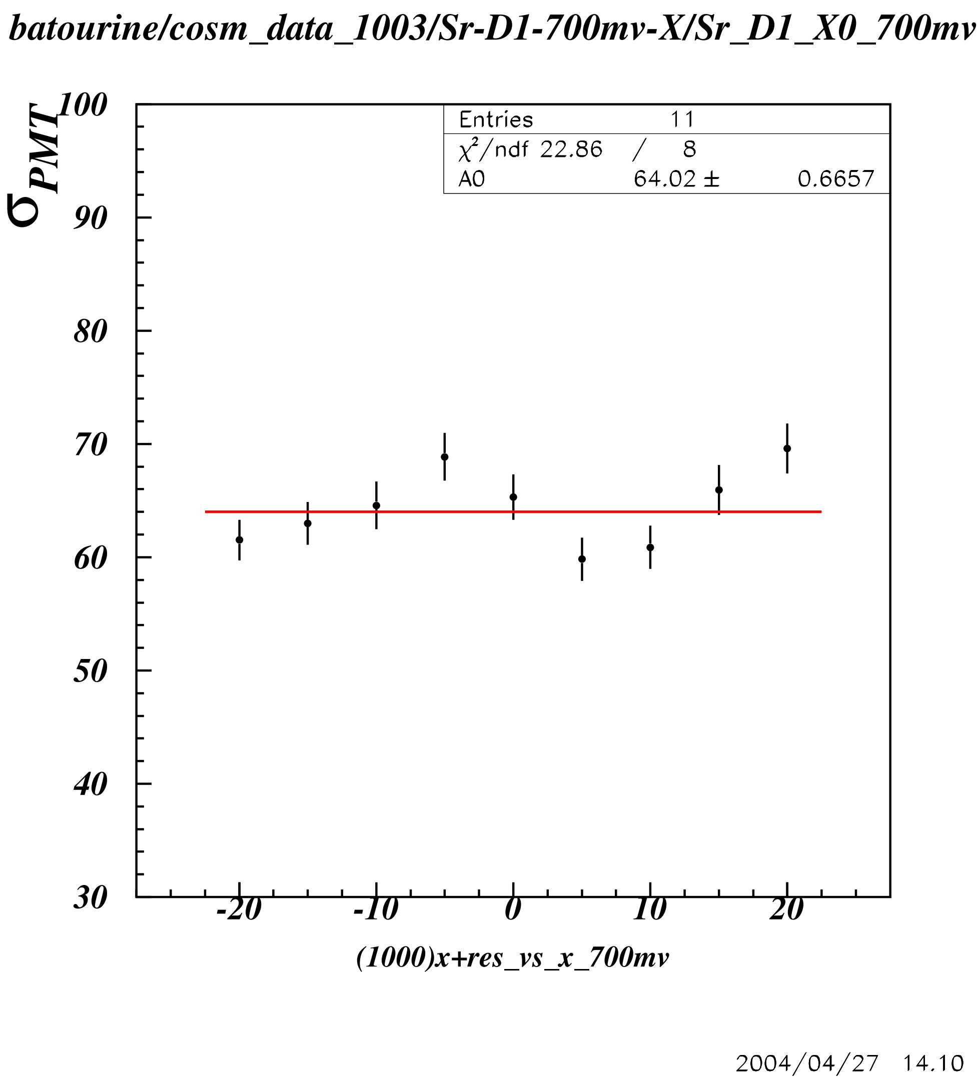

Figure 7: The dependence of σ_{PMT} from $X+$ method upon X-coordinate at $low\ HV = (2200V, 2300V)$.The averaged value is of $64.0 \pm 0.7\ ps$.

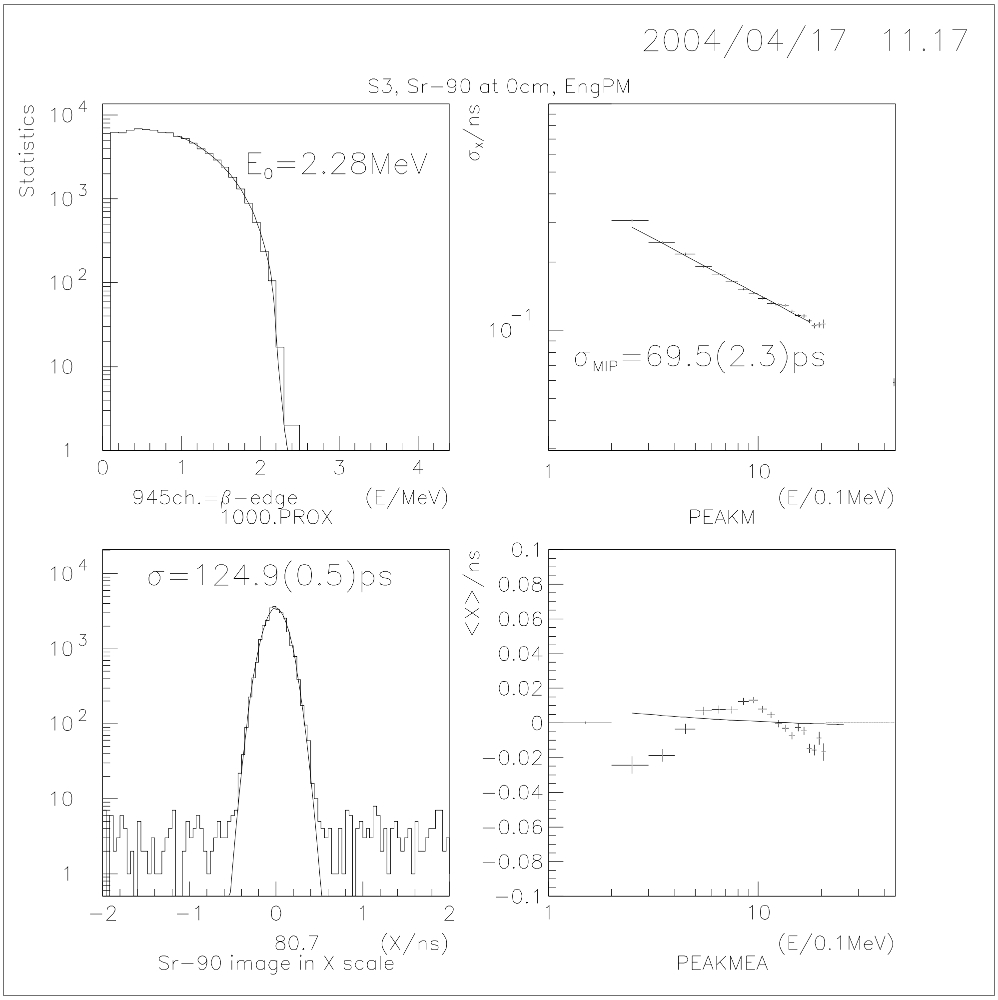

Figure 8: EMI-9813B resolution at *high* HV. Extrapolated to MIP energy σ_{PMT} is of $69.5 \pm 2.$ ps.

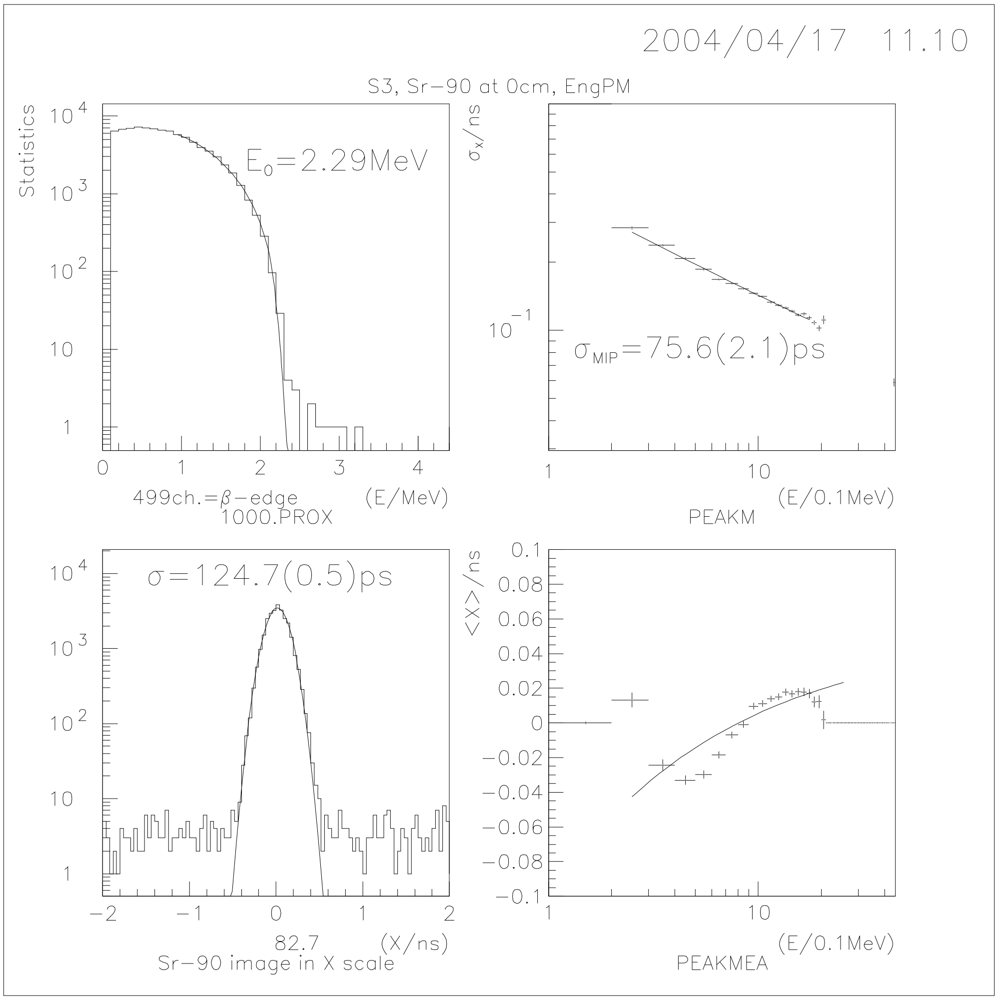

Figure 9: EMI 9813B resolution at *low* HV. Extrapolated to MIP energy σ_{PMT} is of $75.6 \pm 2.$ ps.

due to some X-dependent displacement of the 6 PMT residuals, which may be seen in Fig. 10(2-2). This systematics has to be accounted via universal correction of the individual PMT's timings.

3 Study of resolution and counting rate capability for the Micro-channel Plate Photomultipliers.

We have also measured the resolution of Micro-channel Plate PMs "Burle-85001-501" using the $X+$ method. The amplifier $LeCroy-612A$ has been used for these measurements, since the direct signal from the MCPs is too low for direct discriminating. The setup is shown in Fig. 11 We note that the sence surface of the "Burle-85001-501" assembly is formed by four MCPs. First we performed the resolutution tests with four MCPs connected to the input circuit in parallel. In this case the effective square of the cathode is almost equal to the size of our scintillator. Then we repeated our tests with only one of four MCPs feeding the input circuit. We find no difference between two measurements. Thus the individual transition times and time deviations for MCPs inside the assembly may be considered equal. We emphasize that according to its data sheet the photo-cathode sensitivity of $Burle-85001-501$ lies between 40 and 55 μA/lm. This value is about twice lower than that for $R2083$ PM of Hamamatsu. Therefore the number of primary photoelectrons has to be at least twice lower and one can expect the timing resolution of MCP PM to be of $\sqrt{2}$ times worse. The typical sample of the coordinate method yield is shown in Fig. 12. Both the $\sigma(2.3\ MeV)$ and $\sigma(4.4\ MeV)$ are about twice higher of values for $R2083$. Since the single electron time resolution of MCPs is very good then the possible reasons for the worse resolution are: (1) noise of preamplifiers (2) statistical fluctuations of primary photoelectrons. The first option may be verified in future with the another type of preamplifier. It has to be located as close as possible to the MCP output (on-board PM such as described in Ref. [4]). The second option may be checked by measuring the number of primary photoelectrons.

Number of primary photoelectrons in MCP. We have measured the number of primary photoelectrons using the same method as for the PMs from Hamamatsu. The result of this measurement is shown in Fig. 13.

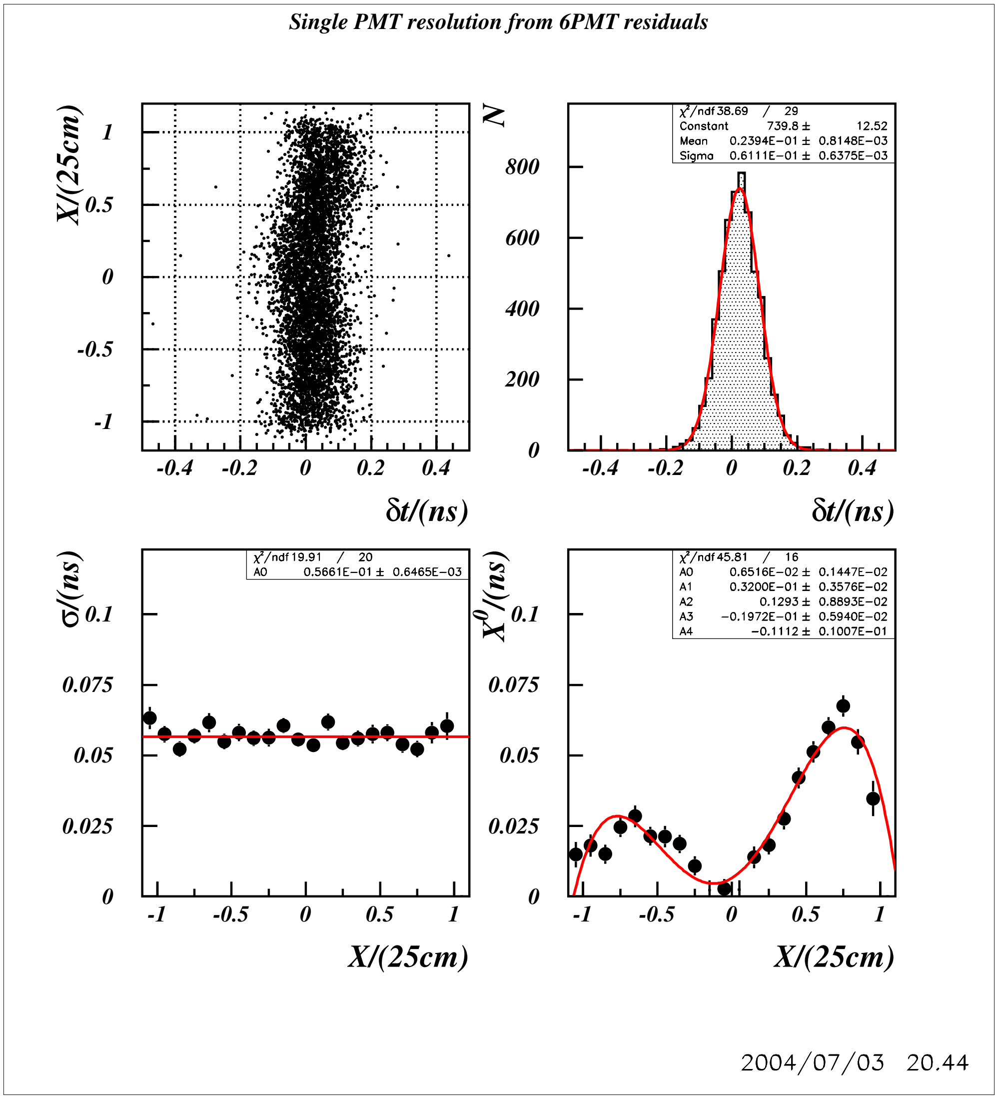

Figure 10: Effective PMT resolution from the 3 counter method.
(1-1):Scatter plot of 6 PMT residuals δt vs X-coordinate.
(1-2):Distribution of 6 PMT residuals (δt).
(2-1):PMT resolution σ vs X-coordinate.
(2-2):Mean value of δt distribution X^0 vs X-coordinate.
Overall σ_{PMT} is of 61.1 ± 0.6 ps. Local σ_{PMT} is of 56.6 ± 0.7 ps.

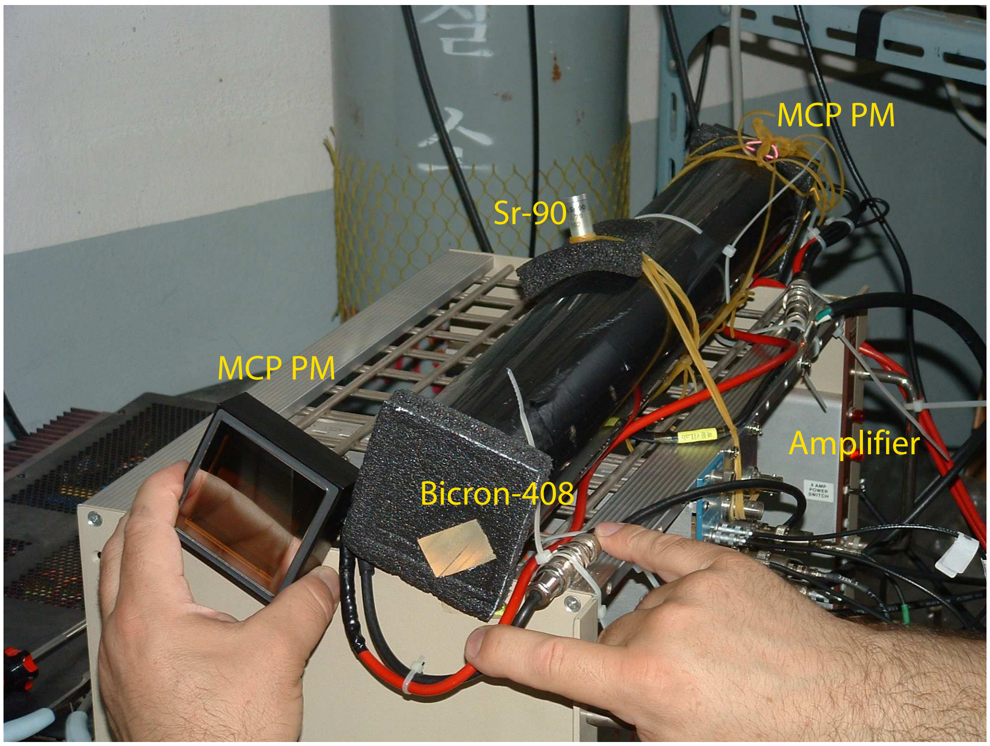

Figure 11: Photograph of the MCP setup.

The extrapolated $N_{ppe}(4.4\ MeV)$ for these samples of MCPs was found to be of 118 ± 10. This value is 5.8 times lower compared with the result for R2083 photomultiplier and about 2.9 times lower of the expected (from the data sheet) value. We note that the second power of the ratio of the MCP PM resolution to the R2083 resolution is of ≈ 5.4(see Table 1). The last number is in agreement with the above mentioned ratio of N_{ppe} numbers of corresponding PMs. Thus, our measurements look consistent.

Measurements of MCP gain. The MCP gain has been determined via the measured N_{ppe} and the charge spectra of β-particles measured via ADCs. Thus measured gain as function of the MCP voltages is shown in Fig. 14. We remind that the voltages have been tuned to provide equal amplitudes from two sides of the detector.

Study of timing resolution vs MCP gain. We have measured the effective resolution of MCPs (PM Burle-85001-501) at different HVs and amplification factors $10^0, 10^1, 10^2$ cascading our preamplifiers. The resolution yielded by $X+$ method resolution is shown in Fig. 15 in function of the MCP gain. One can see a plateau between gains 0.4×10^5 and 6.5×10^5, where the extrapolated to M.I.P.s resolution lies in the interval $(102, 132)\ ps$. The leftmost and rightmost points in this figure were obtained at very low output signals(below $5pC$ in ADC scale) with the amplification factors 10^2 and 1 respectively. Therefore we exclude them from consideration.

Counting rate capability of MCPs with Light Emitting Diode. The counting rate capability of these PMs has been measured in following way. The radiative source was replaced by the Light Emitting Diode. This LED has been fed from the pulser $LeCroy - 9210$ with a pulse of $5V$ amplitude and controllable width $50 < \tau < 100\ ns$. From the scope measurements the rise time of the light signal(i.e. of the PM current) was found to be equal to τ. Therefore timing measurements with $X+$ method with LED makes no sense, since the distribution is very wide(of about 20 ns). However, the signal produced by LED fits well into the ADC gate(200 ns) and reliable ADC measurements of the pulse charge are possible. According to the measurements with a scope the amount of light produced by LED is proportional to τ^2.

We have performed tests for the counting rate capability at two sets of

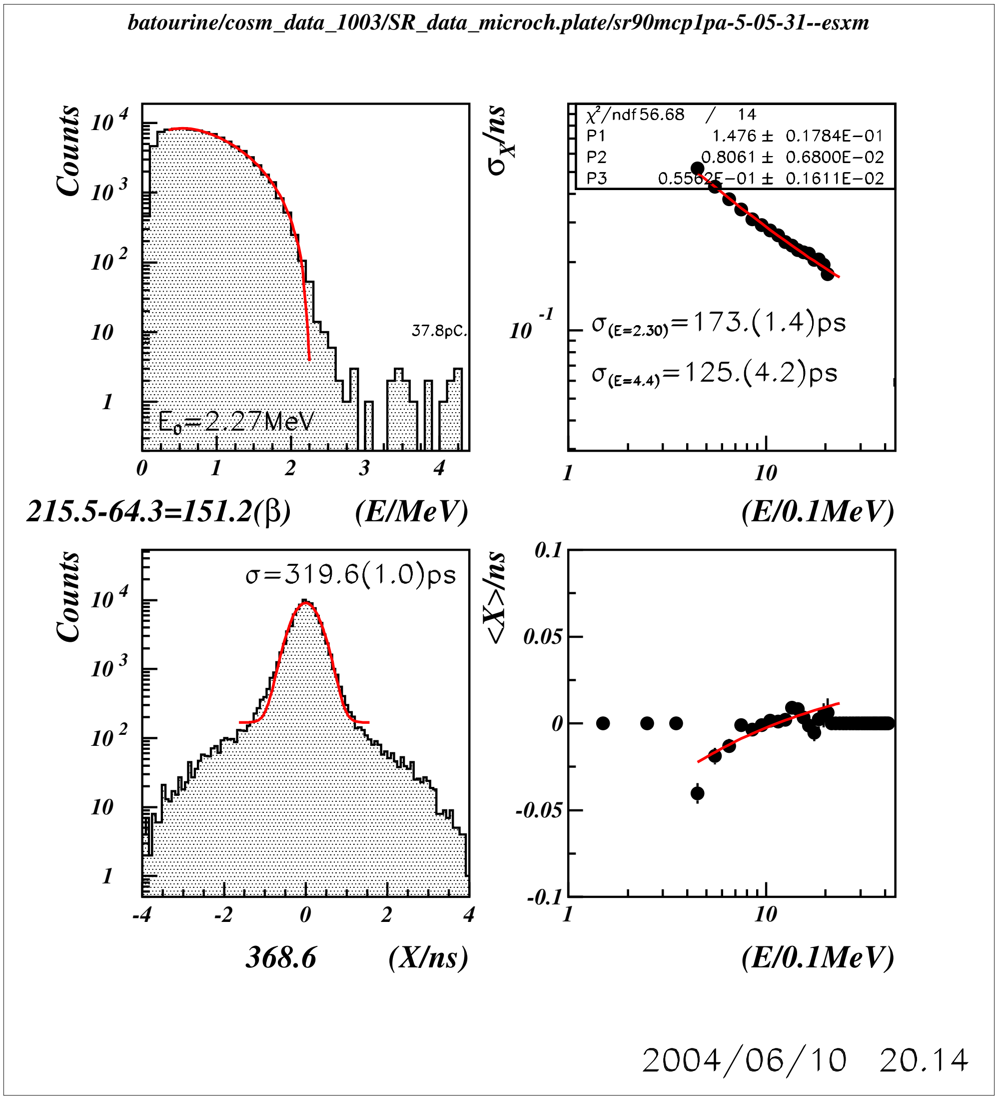

Figure 12: $X+$-coordinate method with MCP PM from "Burle" at highest $HVs = (2150\ V; 2400\ V)$. Extrapolated to M.I.P.s σ_{PMT} is of $125 \pm 4.\ ps$. Amplification factor is of 10^1.

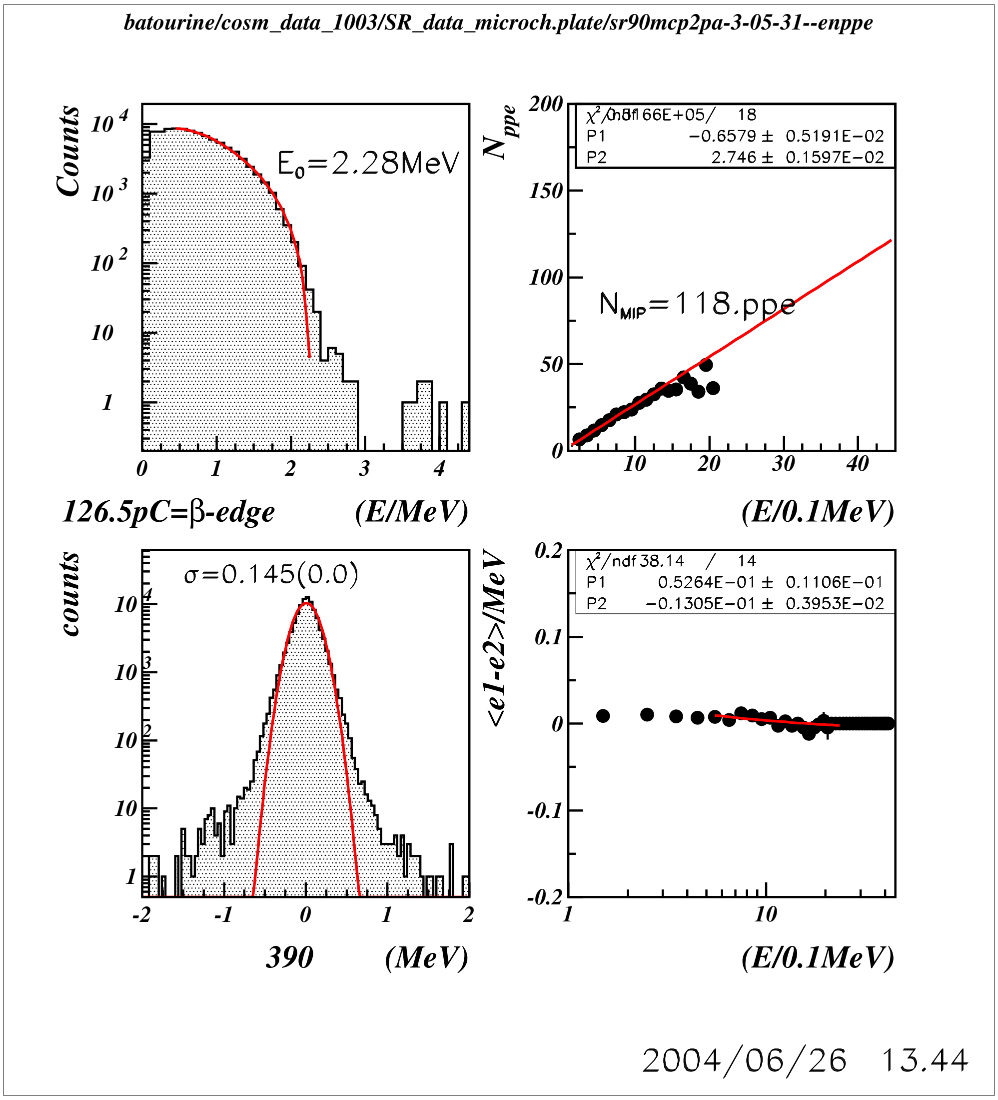

Figure 13: $X+$-coordinate method with MCP PM from "Burle" at $HVs = (1940, 2100)V$. Extrapolated to M.I.P.s N_{ppe}=118 ± 10. Amplification factor is of 10^2.

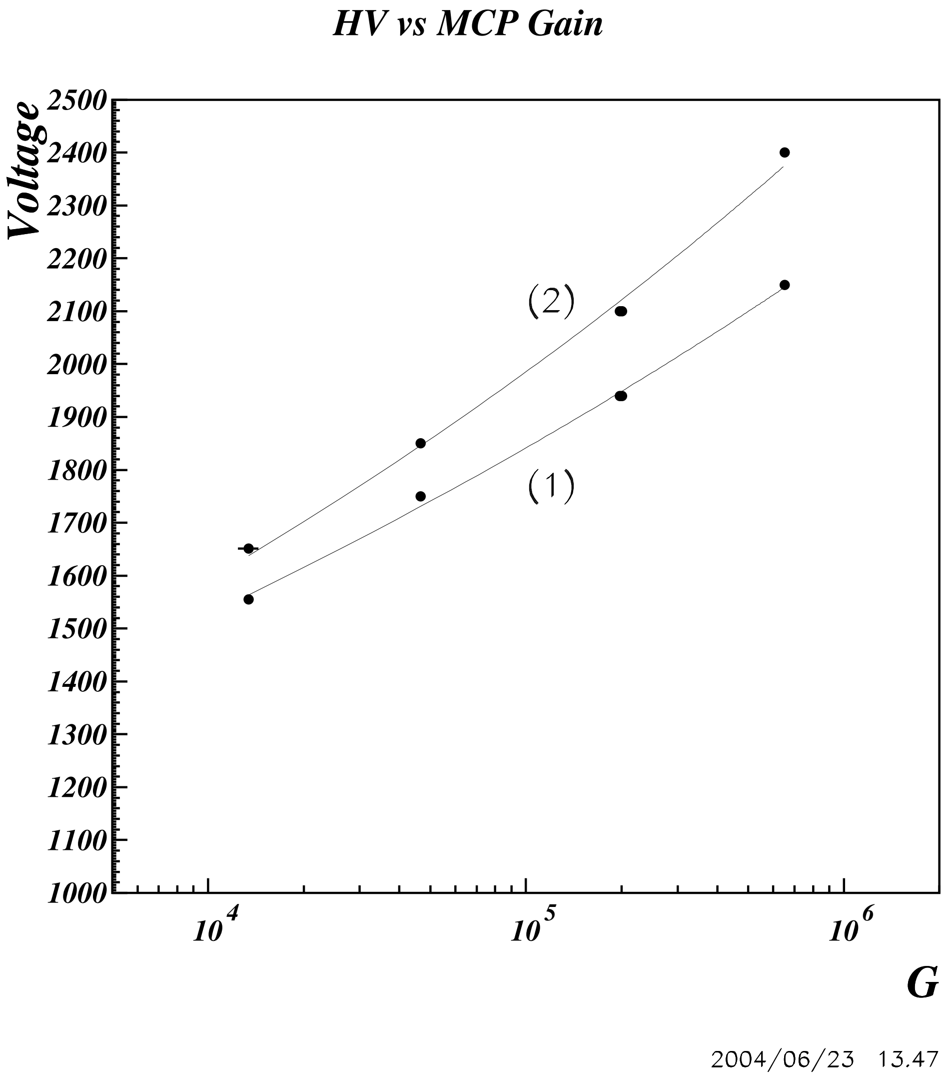

Figure 14: High Voltage vs MCP Gain. The curves (1) and (2) are fits to the power law. (1)-left MCP PM,(2)-right MCP PM.

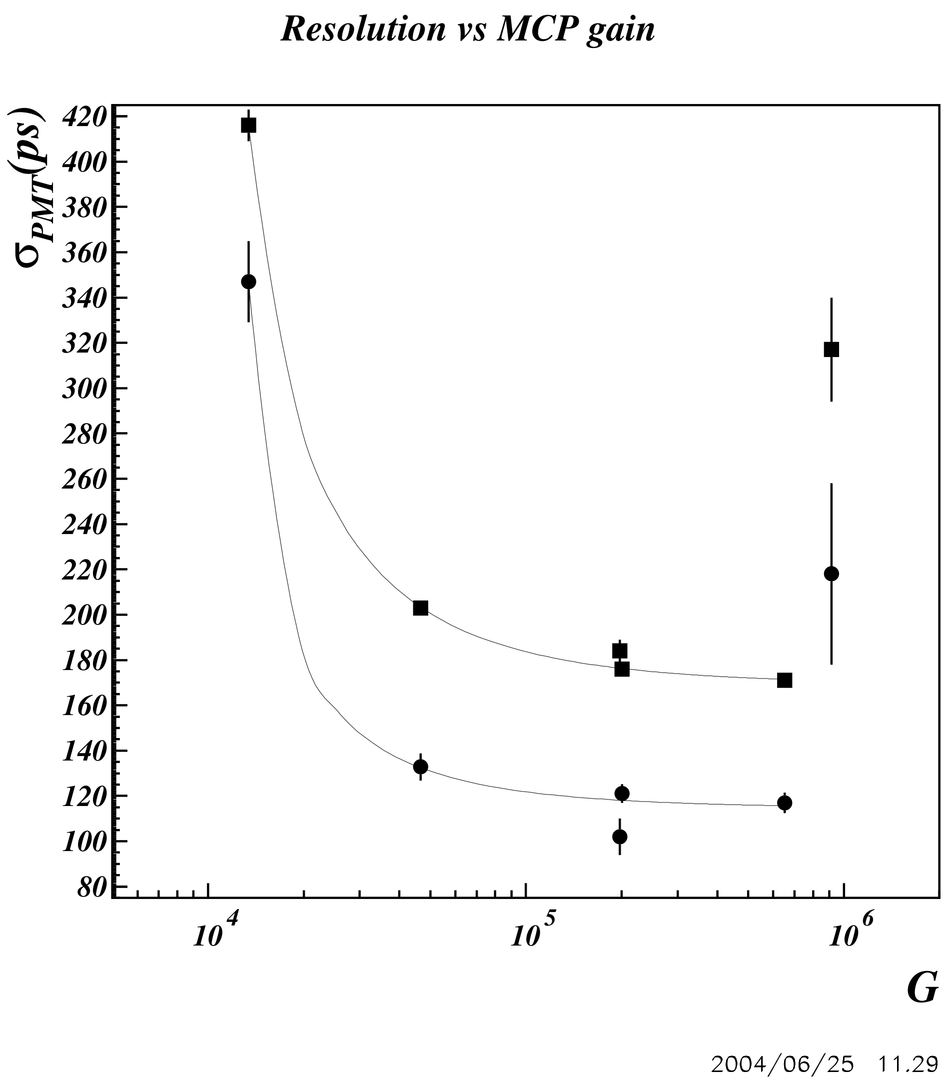

Figure 15: Resolution vs MCP gain(G). Squares are for σ_{PMT} at $\Delta E = 2.28\ MeV$. Circles are for σ_{PMT} extrapolated to $\Delta E = 4.4\ MeV$(M.I.P.s) The curves are fits to the G^{-2} dependence. Amplification factor varies from 10 in the gain region of$(2.0, 6.5) \times 10^5$ to 10^2 in the region $(0.13, 2.0) \times 10^5$. Two points at 2.0×10^5 were measured at amplification 10^1(lower value) and 10^2 for comparison.

HVs= (2400 V, 2400 V) and (1815 V, 1875 V) for the left and right PMs, respectively. At highest HVs we have also taken data at *high* and *low* energies of light flashes, corresponding to τ=100 ns and 50 ns, respectively. The behavior of signal charge vs counting rate is shown in Fig. 16

From the curves (1) and (2) in Fig. 16 one can conclude that the signal charge is proportional to τ^2. The plateau region of curve (3), which was obtained at the gain of $(0.7 \pm .02) \times 10^5$, is much wider than that of curve (1), obtained at the gain of about 6.5×10^5. According to the Fig. 15 the single MCP resolution is of about 130 ps at conditions of the curve (3). Hence, one can conclude that at reduced gain of about 0.7×10^5, provided the amplification factor of 10^2, these MCPs can operate at counting rates up to $.5 \times 10^6$ Hz. The last value corresponds to about 75% of the gain at 10 KHz.

Number of primary photoelectrons from LED. It is important to know the energy of the light flash at the input of the PM. We have estimated the number of primary photoelectrons produced by the LED. Estimates were made from ADC distributions for both left and right PMs in the setup. The samples of ADC spectra are shown in Fig. 17 at the extreme case of very high counting rate of 2×10^6 Hz and highest possible HV of 2400 V for both PMs. Both spectra contain a clear peak corresponding to LED signal. The fitted centroids(sigmas) are 300.0(38.0) and 187.1(16.6) for left and right PMs respectively.

For our estimates of N_{ppe} we have used the data obtained at high voltage and low counting rates. From several measurements we have estimated the total number of primary photo-electrons *produced by LED* as 114 ± 25. This value is close to the N_{ppe} for M.I.P.s, defined from Fig. 13. Therefore, we consider the results shown in Fig. 15 as estimations of the counting rate capability of our MCP setup for scintillations of minimum ionizing particles.

4 Conclusion

In this notes we have confirmed with two different methods that the effective timing resolution of $R2083$ attached directly to the scintillator is better of 60 ps. This value establish the basis for further measurements with $1m$ long light guides. We expect the effective resolution to be significantly worse for such design. Therefore, we are looking for alternatives to this design.

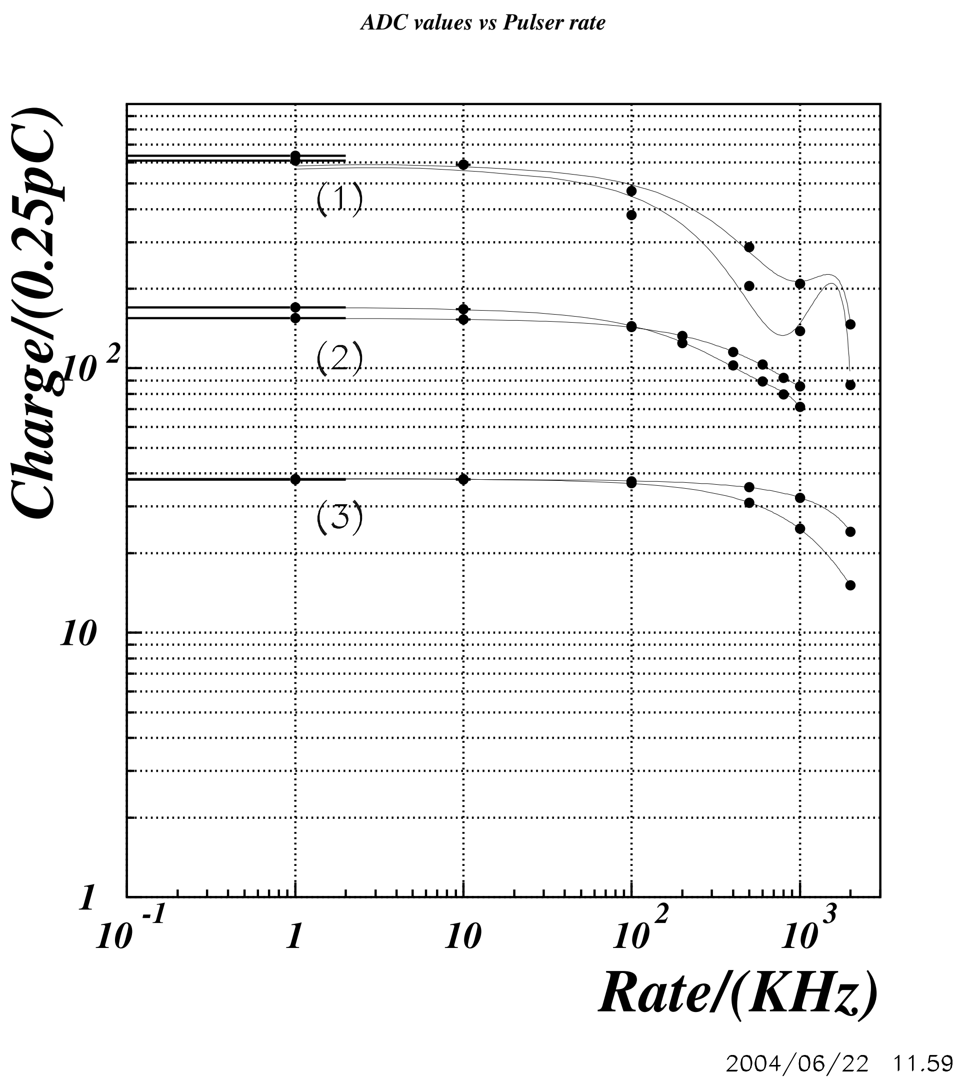

Figure 16: The integrated current of MCP PM signal (ADC counts) vs the rate of light flashes(i.e. pulser rate). The light has been generated by the LED fired via the pulser.
(1)-at HVs=$(2400, 2400)$ V and $\tau = 100$ ns
(2)-at HVs=$(2400, 2400)$ V and $\tau = 50$ ns
(3)-at HVs=$(1815, 1875)$ V and $\tau = 100$ ns
Amplification factor is 10^2 (two cascaded PAs).

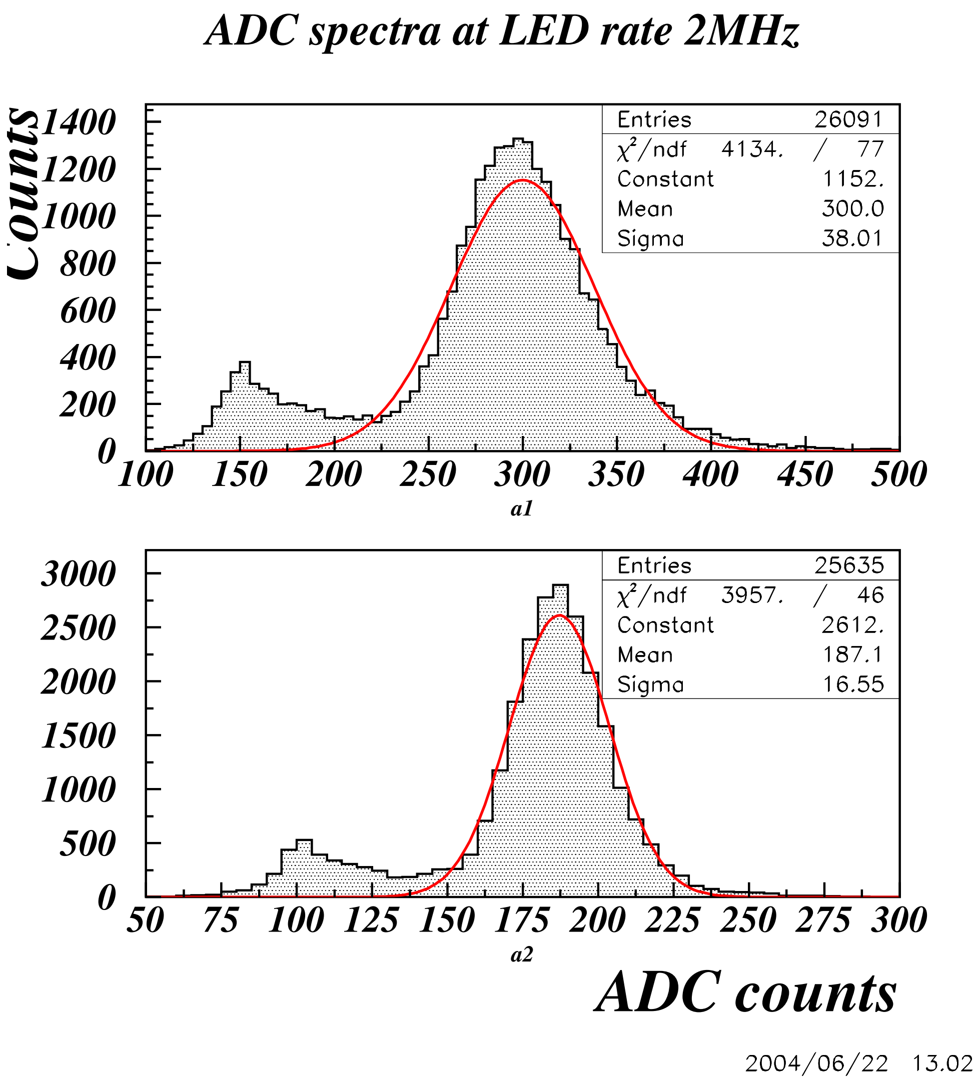

Figure 17: The ADC spectra of MCP PM signals generated by LED at 2 MHz rate. Amplification factor is of 10^2. HVs=$(2400, 2400)$ V,$\tau = 100$ ns.

With this purpose we have estimated the σ_{PMT} for the $Burle$ $85001-501$ MCP PMs, at M.I.P.s energy, as 132 ± 4 ps. This value was obtained at the very low gain of about 4.5×10^4 using an external amplification of 10^2 to the PM's signal. We have shown that at this gain the counting rate of M.I.P.'s scintillations can be as high as 0.5 MHz. Also we have estimated the expected number of primary photo-electrons produced by M.I.Ps in the MCPs. This number is 2.9 times lower than the value expected from the $Burle-85001$ data sheet. The same method of estimating N_{ppe} gives the reasonable number for the $R2083$ PMs of Hamamatsu. Therefore, we may expect that σ_{PMT} of $Burle-85001$ MCP PM would be 1.7 times better ($i.e.$ ≈ 77 ps) for samples with the declared sensitivity of the photo-cathode. In this case the timing resolution of $Burle-85001$ could be significantly closer to the requirements of CLAS experiment at $12GeV$. Its counting rate capability with external amplification of 10^2 is also quite close to the typical counting rates of CLAS experiments.

However, we do not preclude that our results on N_{ppe}, obtained with amplifiers, are biased and that real N_{ppe} corresponds to the data sheet. Therefore, it would be very helpful to measure, independently, the sensitivity for each sample of MCP PMs.

Our preliminary study of MCPs shows that performancr of $Burle-85001$ is quite close to the extremal experimantal requirements of CLAS experiments. Nevertheless, it is clear that the counting rate capability of MCP PMs may be improved. One of the possible ways for that is by means of implementation of Wide Dynamic Range MCPs such as F6584 from Hamamatsu. Photomultipliers instrumented with such MCPs could operate at significantly higher counting rates and/or gains. Thus, we plan to propose to one of the photonics company to design such photomultipliers.

References

[1] E.S.Smith et al., "The time-of-flight system for CLAS", Nucl. Instr. and Meth. A **432**,265-298 (1999).

[2] CLAS-NOTE 2004-16(JLAB, 2004).

[3] H. Kichimi et al., "Timing characteristics of micro-channel plate and fine mesh photomultiplier tubes in a 1-Tesla field", Nucl. Inst. Meth. A **325**, 451 (1993).

[4] V. Popov, “Design And Study Of Photomultiplier Pulse-Shaping Amplifier Powered By The Current Flowing Through A Voltage Divider,” Nucl. Inst. Meth. A **505**, 316 (2003).